

## Numerical Analysis of GNP/Ag Die-Attach Adhesives with Different Thermal Conductivity

Ameeruz Kamal Ab Wahid<sup>1</sup>, Mohd Azli Salim<sup>2,3\*</sup>, Nor Azmmi Masripan<sup>2,3</sup> Chonlatee Photong<sup>4</sup>, Adzni Md. Saad<sup>2</sup>, Mohd Zaid Akop<sup>2</sup> and Muhd Ridzuan Mansor<sup>2</sup>

<sup>1</sup>Jabatan Kejuruteraan Mekanikal, Politeknik Sultan Azlan Shah, Behrang Stesyen, 35950 Behrang, Perak, Malaysia

<sup>2</sup>Fakulti Kejuruteraan Mekanikal, Universiti Teknikal Malaysia Melaka, Hang Tuah Jaya, Durian Tunggal, 76100 Melaka, Malaysia

<sup>3</sup>Advanced Manufacturing Centre, Universiti Teknikal Malaysia Melaka, Hang Tuah Jaya, 76100 Durian Tunggal, Melaka, Malaysia.

<sup>4</sup>Graduate School, Mahasarakham University, Khamriang Sub-District, Kantarawichai District, MahaSarakham 44150, Thailand

### ABSTRACT

*The thermal conductivities of a multilayer model of GNP/Ag hybrid die-attach material are explored using steady-state thermal modeling. The heat flux in multilayer GNP/Ag hybrid structures is shown to be highly layer number dependent. It rises when thermal conductivity increases while density and specific heat value remain constant. For FEA analysis, six different thermal conductivity of GNP/Ag hybrid die-attach materials models were developed to compare with baseline findings from another researcher. By evaluating the total heat flux, FEA modeling was utilized to identify how the increase of thermal conductivity had affected the die-attach materials model. Fourier's law of heat conduction was implemented to investigate thermal characteristics during heating with commercial software code, namely ANSYS. Temperature dependency and thermal material properties, and other thermal parameters boundary conditions were taken into consideration throughout the thermal conductivity procedure. The total heat flux distribution changes of dies with die-attach and substrate assemblies were obtained and thermal characteristics were analyzed during heating within 1 second by using temperature load, 90.3 °C on the dies (diode) surface. Moreover, heat flow and material resistance were also manually calculated in the model by comparing the relationship discovered in the die-attach materials. GNP/Ag hybrid with the highest thermal conductivity, 300 W/m.K, offered the highest heat flux value in terms of simulation,  $7.081 \times 10^6$  W/m<sup>2</sup>, and calculated,  $24.695 \times 10^6$  W/m<sup>2</sup>. As a result, material resistance and heat flux were inversely proportional, and as material resistance reduced, so did heat flux or heat conduction on the material. Thermal conductivity values discovered on die-attach materials can also be utilized to demonstrate the similarities between thermal and material resistance.*

**Keywords:** GNP/Ag Hybrid, die-attach materials, steady-state thermal, thermal resistance, total heat flux

### 1. INTRODUCTION

Thermally conductive adhesives have a wide range of applications in the electronics industry. Bonding SMDs (Surface Mount Devices) to substrates, bonding heatsinks for dissipating heat from circuit boards or other components, and potting and encapsulating parts are some of the most common applications (including PCBs, transformers, and coils). Electric motors, batteries, lighting, and LED heat transfer management all have applications that can be utilized in a variety of applications where good heat transfer between parts is required, such as heating and cooling units (heat exchangers), tooling, and mechanical parts. When soldering isn't an option, thermally

conductive adhesives are an excellent alternative. They can also be utilized to replace the mechanical assembly, saving cost and resources while also reducing component weight and preventing rattling and vibration loosening. Metallic core nanoparticles are known to have excellent thermal conductivity because metal solid particles have a small inter-atomic gap, making thermal conduction easier [1]. Because of their strong thermal conductivity, electrical conductivity, mechanical strength, charge carrier mobility, an extraordinarily large surface area, carbon-based nanoparticles are the most commonly used materials [2].

Die-attach adhesives are essential not only for semiconductors or circuit boards structural stability but also for heat control and improved electrical performance. The die-attach layer has the most important impact on the thermal performance of high-power LED modules because it is the inevitable thermal transfer medium from the chip to the substrate or heat sink [3]. Heat dissipation, mechanical support, and electronic conductivity are all key functions of the die attach solder layer [4]. Heat dissipation is now one of the difficulties preventing multi-heat source power sources from gaining general acceptance [5]. Nanofluids' ability to improve heat transmission has prompted researchers to develop concepts and technologies that are being advocated by manufacturers of ultra-compact, downsized, and intrinsic electronic chips [6]. In order to meet the requirements of high-temperature power electronics applications, specific die-attach materials are a real concern. As a result, a lot of academics throughout the world are attempting to identify the best materials and procedures for generating high-temperature die-attachments.

Graphene has potential benefits such as excellent electrical and thermal conductivity, and it can be used in electronic circuits in vehicles, especially for driver health monitoring systems [7]. Thermal conductivity, mechanical strength, and electrical conductivity are all improved by graphene particles. Significant research on the utilization of water-based Gr-Ag nanoparticles made by [8] using the same process as [9] has been conducted in recent years. The GNP/Ag nanofluid hybrid was prepared by dispersing the nanocomposite in distilled water without the use of a surfactant or ultrasonication, and the researchers discovered that the nanofluids were stable and that no sedimentation occurred for a long time. In comparison to the base-fluid, the experimental data for GNP-Ag nanofluids showed improvements in effective thermal conductivity and heat transfer efficiency [8]. According to [10], graphene nanofluids had a better thermal conductivity enhancement than other nanofluids tested. Graphene has excellent thermo-physical characteristics, making it a good option for application in nanofluids [2].

The research work aimed to demonstrate the comparative difference in material resistance and total heat flux caused by changing the thermal conductivity of the GNP/Ag hybrid. The material properties; density and specific heat from [8] were used as input parameters for material properties in FEA modeling. The differential in material resistance and total heat flux during stretching could also be optimized by determining the fatigue in different pattern lines. Experimental results from [8] were used as the input parameters for material properties in FEA modeling to compute the total heat flux. The study's goal was to assess the dependability of the GNP/Ag hybrid material at various thermal conductivity values, as well as the model's condition at the thermal weak point, and to determine how different values of thermal conductivity create considerable heat flow variance that can be quantified using the total heat flux obtained by FEA modeling.

The material properties of die-attach materials must be recognized. Different thermal conductivity values will have a substantial thermal effect on the results, and FEA analysis was used to investigate the effect of die-attach materials on total heat flux. However, there is a lack of information on the thermal dissipation produced by attachments, as well as the impact of different die-attach materials and toughness on thermal dissipation. The steady-state thermal analysis can be used to optimize the maximum total heat flow during heating. Following the accomplishment of the above objective, an attempt was made to discover the optimal GNP/Ag hybrid die-attach materials with the lowest total heat flux as determined by FEA modeling.

## 2. METHODOLOGY

The objective of this research was to find out which thermal conductivity of GNP/Ag hybrid die-attach materials had the least amount of total heat flux. The thermal conductivity of the GNP/Ag hybrid has been increased to see how heat conduction affects the FEA model. The circuit's time-dependent behavior was next investigated using the lowest numerical results. Numerical workbench tools were used to perform the circuit's FEA. Circuits were constructed in CATIA modeling software, then converted as IGES files and imported into the workbench. After that, the model was fine-meshed before being confirmed using the tetrahedrons patch confirming method, which was expected to take some time. ANSYS steady-state thermal simulation was used to observe the total heat flux of silicon carbide (SiC) diodes that were subjected to temperature loads.

### 2.1 Model Configuration

Material properties from [8] were applied in this research. Material properties studies on density, specific heat, and thermal conductivity of GNP/Ag hybrid, as well as simulated total heat flux values were used. As illustrated in Figure 1, the model was constructed in CATIA, then saved in IGES format and imported into the workbench software. By utilizing ANSYS to apply temperature load values on the dies, a thermal analysis was performed to investigate the total heat flux variation across the model layers. Die-attach was the adhesive or connector that linked the substrate to the diode (die). Copper was used as the model substrate, and silicon carbide (SiC) diodes were directly bound to it using die-attach techniques.

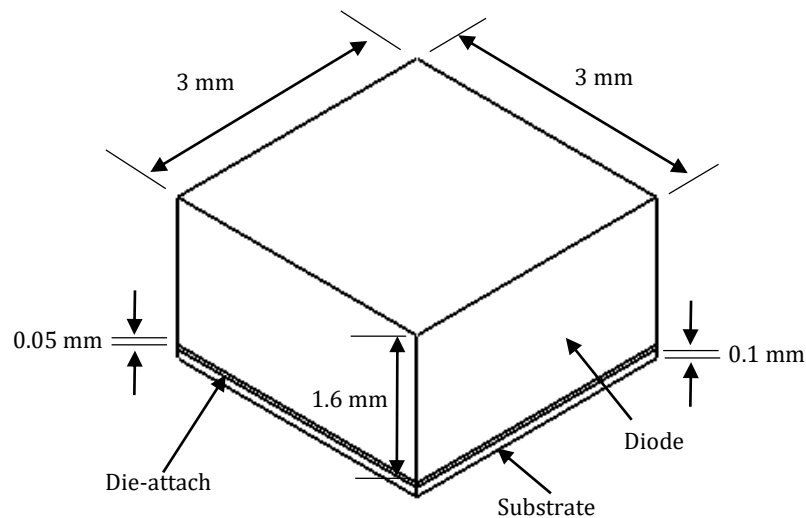


**Figure 1.** Isometric view of FEA model with dimension.

### 2.2 The Finite Element Analysis

The analysis was followed by employing a mesh-generated finite element technique to numerically solve the governing equations at each node. The fine mesh option with the tetrahedrons patch confirming (TPC) method was utilized with the model preference, as indicated in Figure 2, and the computation required some time. There were 44,592 nodes and 24,341 elements in the finite element model.

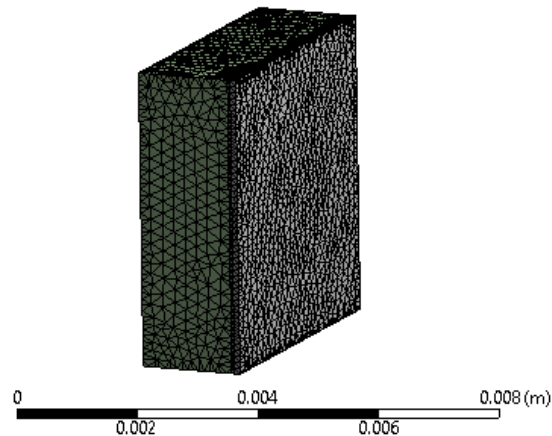


**Figure 2.** Mesh model of the die-attach sample.

The circuit's thermal behavior under heating load was simulated using FEA of conductive inks thermal analysis on a model using ANSYS software. To mimic the screen-printing approach, the die-attach was modeled as a layered structure. The goal of the research was to determine how different die-attach materials affected heat transfer between the diode and the substrate. The goal of this study was to determine which thermal conductive GNP/Ag hybrid die-attach materials are appropriate for the entire model based on the lowest total heat flux maximum values.

### 2.3 Boundary Conditions

The simulation began by identifying the materials that comprised the model, as well as their important physical parameters such as thermal conductivity, specific heat, and density. The devices were silicon, the circuit substrate was copper, and the lands on the circuit were die-attach. Using [8] as a reference, six distinct thermal conductivity GNP/Ag hybrids were created without changing the density or specific heat of die-attach materials' properties. This study used [11] as a reference for the maximum temperature performed on semiconductor devices, diodes. The researcher first attempt to establish simulation baseline findings produced maximum temperatures ranging from 37.3 ° C to 38.3 ° C on SiC dies using metallic die-attach materials and a maximum temperature of 90.3 ° C on the die with epoxy die-attach. Because epoxy had substantially lower thermal conductivity than metallic die-attach materials, it caused higher temperatures on the SiC diodes than metallic die-attach materials.

In a thermal analysis, temperature and other thermal parameters vary over time and are used to evaluate structural analyses in steady-state thermal research. The induced loads are time functions that can be utilized to partition the load versus time curve into load phases in the thermal analysis [12]. The SiC dies were selected as a source of volume heat. To compare thermal conductivity between all die-attach materials, a maximum temperature of 90.3 ° C was applied to SiC dies with GNP/Ag hybrid die-attach materials at 1 second.

### 2.4 Die-attach Properties

Conductive adhesives are suitable for mounting temperature-sensitive chips on substrates because their curing temperatures are significantly lower than soldering temperatures. Furthermore, these adhesives are far more flexible than solder and hence better equipped to endure substrate bending. Another advantage of conductive adhesives over soldering is that they are lead- and solvent-free. Die-attach also offers thermal and/or electrical conductivity between the die and the package, influencing the device's performance while in use. As a result, selecting the best die attach material for a semiconductor device and application is critical. Table 1 shows [8] findings that were utilized as a baseline input and other material properties for FEA modeling

to compute the total heat flux. The values differed from the material properties used in this paper, as obtained from previous and other researchers. Water-based Gr/Ag was identified as GNP/Ag 1 used in this research as a result of the finding [8].

**Table 1** Material Properties Used for Simulation Analysis

Materials	Properties			
	Density (kg/m <sup>3</sup> )	Thermal Conductivity (W/m.K)	Specific Heat (J/kg-K)	Reference
GNP/Ag 1	997.9	0.698	378.57	[8]
Copper	8300	401	385	[13]
SiC (Diode)	3215	120	650	[14]

Using [8] as a reference in the material properties of GNP/Ag hybrid die-attach, the die-attach domain was divided into 6 samples with ascendingly increased thermal conductivity starting at 50 W/mK and increasing to 300 W/mK with each sample interval representing 50 W/mK without changing the data on density and specific heat. Table 2 shows the material properties used in the FEA simulation analysis, from GNP/Ag 2 to GNP/Ag 7, which represented the new thermal conductivity of die-attach materials.

**Table 2** Calculated Material Resistance and Heat Flux of Samples Die-Attach Materials

Material	Thermal Conductivity (W/m.K)
Gr/Ag 2	50
Gr/Ag 3	100
Gr/Ag 4	150
Gr/Ag 5	200
Gr/Ag 6	250
Gr/Ag 7	300

## 2.5 Heat Flux

The rate of thermal energy flow per unit surface area of the heat transfer surface is known as heat flux. To evaluate thermal conductivity between all die-attach material models, heat flux was applied to the SiC dies surface with die-attach materials within 1.5 seconds. On different die-attach models, the total heat flux can be calculated using Equation (1). Fourier's law of heat conduction [15] can be used to calculate the heat flux:

$$q'' = k (dT/dx) \quad (1)$$

where 'q' represents heat flux (W/m<sup>2</sup>), 'k' and 'dT' are the thermal conductivity coefficient (measured in W/m °K) and temperature of heat applied to the top surface of the diode (measured in Kelvin), respectively, and 'dx' stands for material thickness (from the top surface of the diode to the bottom surface of the substrate).

The R<sub>1</sub>, R<sub>2</sub>, and R<sub>3</sub> represent the diode, die-attach, and substrate, respectively, in Figure 3(b). The load given to the diode flows through these three layers of resistance. The heat is transferred from the diode through the die-attach, substrate, and eventually to the surrounding temperature of 24 °C to obtain the overall heat flux values of the model. The calculated total heat flux value and the ANSYS simulated total heat flux value were compared. Material resistance, R, was provided by the

following equation, as shown in Figure 3(b):

$$R = \frac{dx}{k} \tag{2}$$

where 'dx' is the material thickness and 'k' is the thermal conductivity of the material. Figure 3 illustrates a schematic diagram of the model's heat flows.

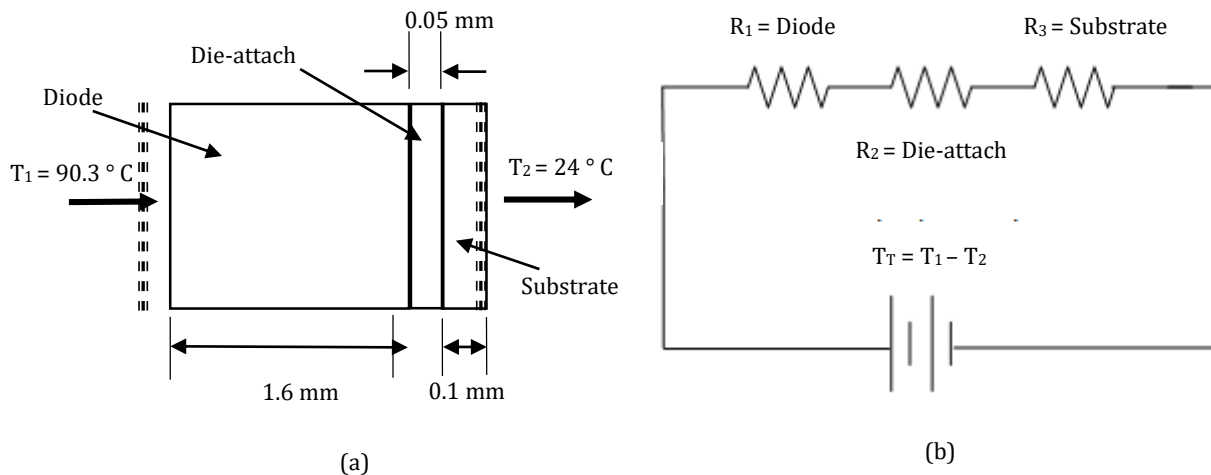


**Figure 3.** Schematic diagram of; (a) heat flows in the model and (b) Heat conductance in the circuit.

## 2.6 Thermal Resistance

Thermal resistance is a useful approach to view and study various heat transfer difficulties using an electrical analogy. The materials' thermal resistance (R) and thermal conductance (C) are reciprocals of one another and can be calculated using thermal conductivity (k) and thickness. According to [16], the heat conductivity of the die-attach layer is influenced by its thickness. As the thickness of the die-attach material reduces, the material's heat resistance falls. According to Equation (3), a material's thermal resistance is proportional to its thermal conductivity coefficient, heat transfer area, and thickness.

$$R_{Th} = \frac{L}{kA} \tag{3}$$

The  $R_{Th}$  stands for thermal resistance, k and A for thermal conductivity coefficient and heat transfer area, and L for die-attach material thickness, respectively. The value of thermal conductivity derived from the simulation result for each die-attach material was validated using the thermal resistance obtained from the manual calculation based on Equation 3.

## 3. RESULTS AND DISCUSSION

### 3.1 Numerical Results

The modeling approach obtained the best simulation results, accounting for the circuit's ambient temperature of 24 °C. Figure 4 depicts a surface plot of the model's calculated surface total heat flux after 1 second of heating. Before delving into mesh and time refinement, as well as the variable thermal conductivity of die-attach models, it is necessary to present heat flow within the model within 1 s. The steady-state thermal on the dies within 1.0 s when using the TPC method in ANSYS is presented in Figure 4. The thermal data divergence occurs when the temperature spreads to the entire model and the reaction is illustrated as the color contour change on the models. Total heat flux or heat flow rate intensity results as shown in Figure 4 is a flow

of energy per unit of area per unit of time in the circuit. The heat flux becomes higher after the time and temperature are increased.

The simulation begins at 24 ° C, which is the ambient temperature, and concludes at 90.3 ° C after 1 second. The adaptive time-stepping method was implemented in all seven die-attach materials models. The heat flows on the dies through die-attach materials to the substrate until 1 s show a change in the color contour on the surface of the circuit model. Figure 4 illustrates that the generated heat on the diode surface has little effect on the color contour of the model. This gives the impression that the model's state is unaffected by the increase of overall heat flux. The color contour appears to change in Figures 4 (a) and (b) as the large difference between thermal conductivity in both model properties. The maximum value is highlighted in red color and the minimum value is highlighted in blue. However, the blue contour plots in Figure 4 (a) seem to disappear in Figure 4 (b), even though the total heat flux value increases and the green contour increases. This means that the heat capacity in the model's mass cannot release heat as a result of the temperature applied to the model.

Table 3 indicates the heat flux and material resistance of calculated and simulation results from the die-attach materials. All calculated heat flux values for each die-attach material increase as the thermal conductivity of each die-attach material increases. Similarly, the material resistance of each die-attach material is found to decrease, indicating that improved thermal conductivity has the impact of better-allowing heat through the material. Table 3 also reveals that the calculated  $24.695 \times 10^6 \text{ W/m}^2$  of heat flux and simulation  $7.081 \times 10^6 \text{ W/m}^2$  of heat flux for GNP/Ag 7 are the highest compared to the other samples. This clearly illustrates that by increasing the thermal conductivity of a material's properties will increase its heat flow rate.

**Table 3** Material Resistance and Heat Flux Results of Die-Attach Materials

Material	Thermal Conductivity (W/m.K)	Material Resistance (°C.m <sup>2</sup> /W)	Calculated Heat Flux (W/m <sup>2</sup> )	Simulated Total Heat Flux (W/m <sup>2</sup> )
Gr/Ag 1	0.698	$71.63 \times 10^{-6}$	$3.984 \times 10^6$	$1.175 \times 10^6$
Gr/Ag 2	50	$1.0 \times 10^{-6}$	$23.284 \times 10^6$	$6.739 \times 10^6$
Gr/Ag 3	100	$0.5 \times 10^{-6}$	$24.11 \times 10^6$	$6.944 \times 10^6$
Gr/Ag 4	150	$0.33 \times 10^{-6}$	$24.399 \times 10^6$	$7.011 \times 10^6$
Gr/Ag 5	200	$0.25 \times 10^{-6}$	$24.546 \times 10^6$	$7.045 \times 10^6$
Gr/Ag 6	250	$0.2 \times 10^{-6}$	$24.635 \times 10^6$	$7.066 \times 10^6$
Gr/Ag 7	300	$0.16 \times 10^{-6}$	$24.695 \times 10^6$	$7.081 \times 10^6$

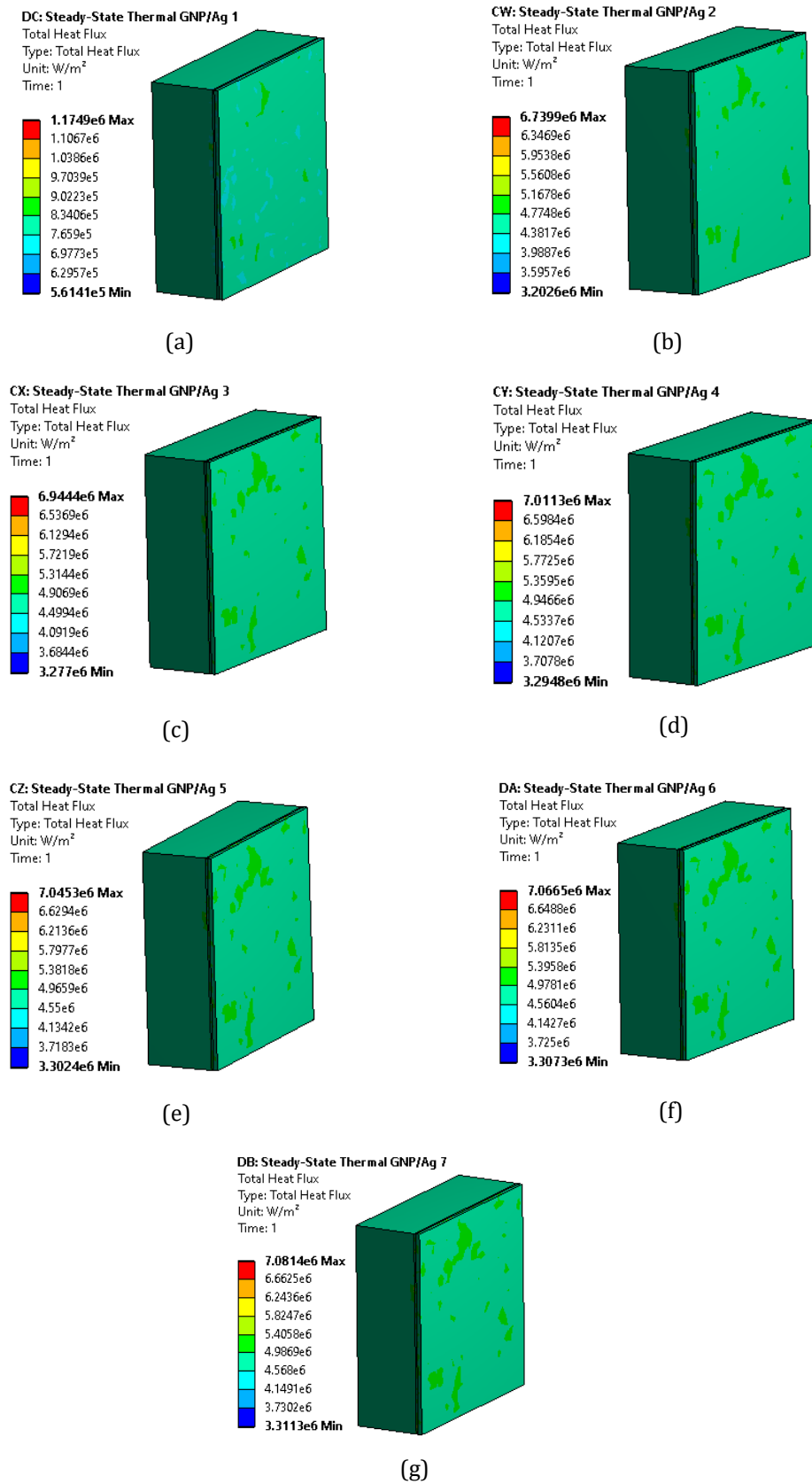
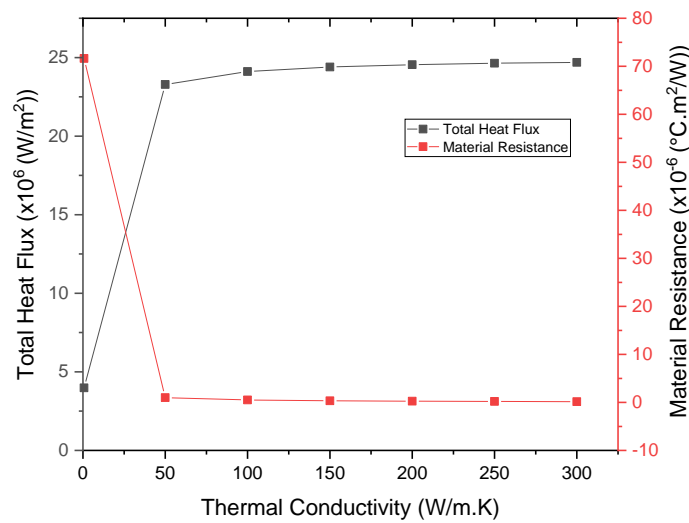


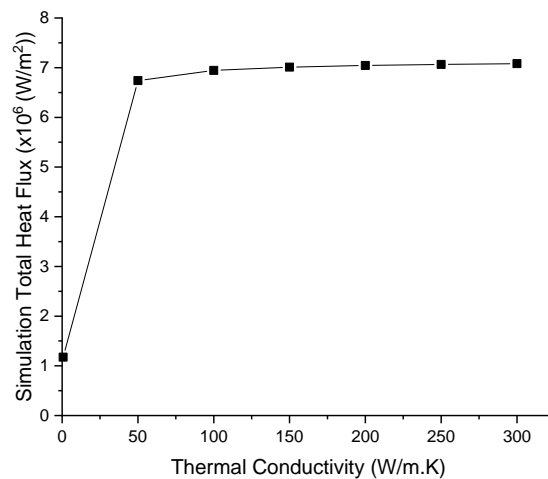
**Figure 4.** Total heat flux results of GNP/Ag hybrid die-attach materials using steady-state thermal analysis. (a) GNP/Ag 1, (b) GNP/Ag 2, (c) GNP/Ag 3, (d) GNP/Ag 4, (e) GNP/Ag 5, (f) GNP/Ag 6 and (g) GNP/Ag 7.



This simulation result can be varied by comparing the calculated total heat flux in Table 3 with the heat flux simulation result, which reveals a little difference. Table 3 shows the heat flux value of the die-attach material generated from numerical simulations to hand-calculated values for convenience. The magnitude of GNP/Ag 1,  $3.984 \times 10^6 \text{ W/m}^2$ , is close to the hand calculated value of  $1.175 \times 10^6 \text{ W/m}^2$ . Figure 5 (a) depicts the relationship between heat flux and material resistance during 1 s of heating at temperatures ranging from 24 to 90.3 ° C. As thermal conductivity increases, all die-attach material heat flux results increase. The heat flux increases significantly from 0.698 W/m.K to 50 W/m.K and then increases slightly with ascendingly higher thermal conductivity until 300 W/m.K, with each sample interval representing 50 W/m.K. Figure 5 (a) also demonstrates that the heat flux is inversely proportional to the material resistance. This means that by lowering the material resistance, the heat flow rate on the materials can be increased even higher.



(a)



(b)

**Figure 5.** Trend of the lines probes during the test, comparison between all die-attach materials specimen. (a) Characteristics of thermal conductivity from the calculation. (b) Total heat flux of simulation.

Figure 5 (b) shows an increase in simulation total heat flux for all die-attach materials during the 1 s heating period. The maximum total heat flux on GNP/Ag 1 die-attach is the lowest of all die-attach samples. This illustrates that GNP/Ag 1 has high thermal resistance after measuring a temperature differential over a die-attach layer material with low thermal conductivity and 0.05 mm thickness. Heat flows more difficultly through the GNP/Ag 1 die-attach due to the high thermal resistance. The graph in Figure 5 (b) shows that with the exception of GNP/Ag 1, all six die-attach materials are close to each other because the results of this thermal investigation are not considered diverse. This is due to the fact that the temperature applied to the diode surface is raised linearly from the beginning of the load at 0 to 1 s.

The layer thickness (few micrometers) of the die-attach materials layer has little effect on the model heat flux conduction, allowing heat to flow more easily [4] [16]. The thermal conductivity of the die-attach layer is the most influential factor in defining a material's thermal resistance. The greater the thermal conductivity, the lower the thermal resistance, and the better the heat conduction of the material. Table 4 shows the significant thermal resistance differences between GNP/Ag 1 and other die-attach because they have different thermal conductivity values even when the die-attach size is the same. As the thickness of the die-attach material drops, so does its thermal resistance. The material's thermal resistance is only a small aspect of the die-attach layer's total thermal resistance [16].

The thermal resistance of a material is inversely proportional to its thermal conductivity coefficient and heat transfer area, as given in Equation 1. This shows that a material's thickness has little effect on its temperature flow rate. Table 4 also shows that the thermal resistance of all six die-attach materials except GNP/Ag 1 is too low and does not differ significantly. It also shows the similarity between thermal resistance and material resistance (Table 3), both of these values reduce as the value of thermal conductivity increases. Because of the use of high thermal resistance die-attach materials, a little amount of heat is spreading across the surface of the circuit. If there is sufficient heat spreading, the diode would have affected the entire circuit, raising the maximum temperatures on the diodes.

**Table 4** Thermal Resistance of Die-Attach Materials

Material	Thermal Resistance (°C/W)
GNP/Ag 1	7.959
GNP/Ag 2	0.111
GNP/Ag 3	0.055
GNP/Ag 4	0.037
GNP/Ag 5	0.028
GNP/Ag 6	0.022
GNP/Ag 7	0.018

#### 4. CONCLUSION

Using steady-state thermal analysis, the study was effective in proving the optimal heat conductivity performance using various thermal conductivity of GNP/Ag hybrid die-attach materials. A modeling approach related to thermal theories was developed to be applied for the varying effects of the different thermal conductivity die-attach materials on the semiconductor device and substrate materials. Among various die-attach materials, GNP/Ag 7 with the highest thermal conductivity, 300 W/m.K, offered the highest heat flux value in terms of simulation, 7.081

$\times 10^6 \text{ W/m}^2$ , and calculated,  $24.695 \times 10^6 \text{ W/m}^2$ . The results of all six die-attach materials, except for GNP/Ag 1, were very similar, which could be due to thermal conductivity and thickness. The heat flux conduction to the model was unaffected by the thinness of the die-attach materials layer. As the thickness of the die-attach material decreased, the thermal resistance tended to fall. The value of material resistance and heat flux were inversely proportional, and as the value of material resistance decreased, so did the value of heat flux or heat conduction on the material. The value of thermal conductivity found on the die-attach material can also be used to prove the similarities between thermal resistance and material resistance.

## ACKNOWLEDGEMENT

Special thanks to the Advanced Manufacturing Centre (AMC) and Fakulti Kejuruteraan Mekanikal (FKM), Universiti Teknikal Malaysia Melaka (UTeM) for providing the laboratory facilities.

## REFERENCES

- [1] Ny, G. Y., Barom, N. H., Noraziman, S. M., & Yeow, S. T. *Journal of Advanced Research in Materials Science*, 22(1), (2016) 11-27.
- [2] Novoselov, Kostya S., Andre K. Geim, S. V. Morozov, D. Jiang, Y. Zhang, SV and Dubonos, I. V. Grigorieva, and A. A. Firsov. *Science* 306, no. 5696 (2004) 666-669.
- [3] Zhang, H., & Sukanuma, K. Springer, Cham. (2019) pp. 35-65.
- [4] Jiang, C., Fan, J., Qian, C., Zhang, H., Fan, X., Guo, W., & Zhang, G. *IEEE Transactions on Components, Packaging and Manufacturing Technology*, 8(7), (2018) 1254-1262.
- [5] Yang, D., Liu, D., van Driel, W. D., Scholten, H., Goumans, L., & Faria, R. *2010 11th International Conference on Electronic Packaging Technology & High Density Packaging*. IEEE. (2010) pp. 1246-1249.
- [6] Zainal, S., Tan, C., Sian, C. J., & Siang, T. J. *Journal of Advanced Research in Applied Mechanics*, 23(1), (2016) 20-35.
- [7] Wahid, A.K.A., Salim, M.A., Masripan, N.A., Ali, M., Saad, A.M., Al-Mola, M.H.A., *International Journal of Nanoelectronics and Materials*, Vol.14 (Special Issue), (2021) pp.373-386
- [8] Yarmand, H., Gharehkhani, S., Ahmadi, G., Shirazi, S. F. S., Baradaran, S., Montazer, E., Zubir, M.N.M., Alehashem, M.S., & Dahari, M. *Energy conversion and management*, 100, (2015) 419-428.
- [9] Sundar, L. S., Singh, M. K., & Sousa, A. C. *International Communications in Heat and Mass Transfer*, 52, (2014) 73-83.
- [10] Babu, J. R., Kumar, K. K., & Rao, S. S. *Renewable and Sustainable Energy Reviews*, 77, (2017) 551-565.
- [11] Ovrebo, G. K. *Thermal simulation of four die-attach materials*. Army Research Lab Adelphi Md Sensors and Electron Devices Directorate. (2008).
- [12] Ravikumar, S., Chandra, P.S., Harish, R. and Sivaji, T., *IOP Conference Series: Materials Science and Engineering*, IOP Publishing. Vol. 197, No. 1, (2017) p. 012085.
- [13] ANSYS Release 16.0 ANSYS Inc., (2015).
- [14] Accuratus Corporation, Silicon Carbide Properties Datasheet, (2013).
- [15] Lienhard, I. V., & John, H. (2005). *A heat transfer textbook*. phlogiston press.
- [16] He, P., Zhang, J., Zhang, J. and Yin, L., *Advances in Materials Science and Engineering*, (2017).